J. Appl. Comput. Mech., 9(2) (2023) 357-370
DOI: 10.22055/JACM.2021.36722.2892

ISSN: 2383-4536
jacm.scu.ac.ir

Shahid Chamran University of Ahvaz

Journal of Applied and Computational Mechanics

Research Paper

Numerical Study on the Ferrofluid Droplet Splitting in a T-junction with Branches of Unequal Widths using Asymmetric Magnetic Field

Mohammad Aboutalebi[1], Mohammad Behshad Shafii[2], Siamak Kazemzadeh Hannani[3]

[1] Ph.D. Candidate, Department of Mechanical Engineering, Sharif University of Technology, Tehran, Iran, Aboutalebi@mech.sharif.edu

[2] Professor, Department of Mechanical Engineering, Sharif University of Technology, Tehran, Iran, Behshad@sharif.edu

[3] Professor, Department of Mechanical Engineering, Sharif University of Technology, Tehran, Iran, Hannani@sharif.edu

Received February 21 2021; Revised August 08 2021; Accepted for publication August 08 2021.
Corresponding author: M.B. Shafii (Behshad@sharif.edu)

Abstract. Research on the microdroplet splitting phenomenon has intensified in recent years. Microdroplet splitting has numerous applications in chemical synthesis, biology, and separation processes. The current paper covers the numerical study of ferrofluid microdroplet splitting at various lengths and velocities inside the T-junction with branches of unequal widths under asymmetric magnetic fields. Microdroplet splitting can be controlled by using an asymmetric magnetic field and the asymmetry in the width of T-junctions branches. Three geometrical models of the T-junction with different widths ratio (0.7, 0.85, and 1), along with a magnetic field with various intensities are studied. This magnetic field is generated by a line dipole. In this study, the distance between the dipole and origin is kept constant. The splitting ratio of ferrofluid microdroplets at different velocities (different capillary numbers), different non-dimensional lengths and different magnetic force (different magnetic Bond numbers) at the center of T-junction are calculated for each amount of branch width. The results are verified with previous works and their correctness is proved. The splitting ratio is defined as the volumetric ratio of the larger daughter droplet to the mother droplet. The results indicate that generally, the stronger the asymmetric magnetic force is, the more asymmetric the splitting will become, with the splitting ratio becoming closer to 1. Also, as asymmetry increases between the widths of the two branches of the T-junction, the splitting ratio approaches 1.

Keywords: Ferrofluid droplets, breakup phenomenon, magnetic field, splitting ratio.

1. Introduction

Microfluidic devices have attracted lots of attention and in recent years, have experienced stunning growth in various varying fields such as the academic and industrial fields [1-9]. Characteristics of microfluidic tools such as controllability, safety, low cost and high productivity encouraged scientists to use them in different industrial equipment [3, 5-8]. The combination of microfluidic flows and magnetic particles can be used in enhancement of heat transfer, separation processes, drug therapies, catalytic reactions, etc. [10-14]

One of the most popular fields of microfluidic studies is the investigation of the breakup phenomenon of microdroplets at micro-junctions [15-20]. In a numerical study in 2009, Leshansky, A. and L. Pismen showed that microdroplets within symmetrical T-junctions could be broken under certain conditions and calculated the minimum length of a microdroplet as a function of the velocity of the microdroplet to breakup in the microchannel [15]. In 2009, Jullien et al. experimentally studied the phenomenon of microdroplets splitting at low-Capillary numbers in symmetrical junctions and observed two different flow regimes of splitting and non-splitting [16]. Bedram and Moosavi also studied the “breakup time” of microdroplets in 2011 while investigating the splitting of microdroplets in symmetrical T-junctions [20]. Symmetrical T-junctions are frequently utilized to breakup microdroplets [15, 18, 20-23]. In this technique, a microdroplet achieves a T-junction with the continuous flows of the main stream. This microdroplet is known as the mother microdroplet. As, the mother microdroplet reached the T-junction, it can be break up into two smaller droplets dependent to the shear forces and surface tension [15, 16, 18, 20, 24]. It should be noted that in this case, if the T-junction is perfectly symmetric (microbranch widths, microbranch lengths, internal roughness of the branches, etc. are perfectly symmetrical) and the microdroplet breaks, each branch of the receptor can accommodate exactly half of the mother microdroplet volume [15, 17, 20, 21, 23]. In this case, the splitting ratio is 0.5, which implies a symmetrical breakup [23]. Also, if the microdroplet inside the purely symmetrical T-junction has not breakup for any reason, the splitting ratio will be 1 [23] (Very low Capillary numbers or very short length of the non-dimensional microdroplet can be factors for non-breakup situation). To increase the possibility of microdroplet breakup, it is suggested to utilize T-junctions with random angles [25] because the sharp edges in the Y-junction allow microdroplets to breakup simply.

Published online: August 11 2021

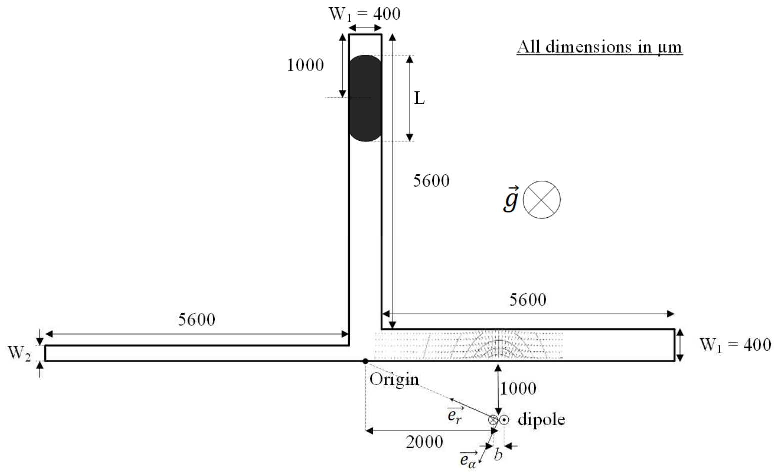

Fig. 1. 2D geometrical schematic of the case utilized in this study. Three geometrical models were used for collecting the results among which only the width of the left branch differs.

Using a symmetrical T-junction can only produce a splitting ratio of 0.5 or 1 [15, 17, 23]. In fact, due to existing symmetry, the splitting ratio can only be 0.5 and 1. On the other hand, it is sometimes necessary to exert more control over the behavior of the microdroplets within the junctions. Sometimes, the microdroplets inside the T-junction need to be broken asymmetrically to produce splitting ratios varying from 0.5 and 1[18, 20, 23, 26]. Compared to the symmetrical splitting into equal-sized droplets, the unequal breakup into unequal-sized droplets has the advantages of reaching precise volume ratio of two smaller droplets and picking up reactants from droplet quantificationally that is crucial in material synthesis and other droplet-operating industries [27, 28].

For this aim, some changes should be considered in geometrical features of T-junction or the initial conditions of models. Therefore, to make changes in geometrical features, the width of the connecting branches, their length, the angle of the branches, etc. can be altered. In this way, the mother microdroplet achieves asymmetric breakup while hydrodynamic resistances of the connecting branches are changed [18, 20, 21, 23, 26]. Bedram and Moosavi in 2011 showed that if the branches' lengths are different, a larger amount of the mother microdroplet goes into the smaller branch after splitting [18]. Also, Salkin et al. in 2013 showed that using obstacle in the microchannel can lead to an asymmetric splitting [21]. Samie et al. in 2013 experimentally depict that if the widths of the microchannel's branches are separate, a larger volume of the mother microdroplet tends to join the bigger part [26]. Moreover, other parameters have impacts on producing various microdroplet sizes inside branches. For example, recent researches revealed that altering the inlet flow rate of the discrete fluid into the continuous one [18, 20, 21, 26], a variation in surface tension between the continuous and separate phases [29], and a change in viscosity [29] can change the performance of microdroplets in T-junctions. Enlarging the flow rate ratio of the separate fluid to the continuous one rises the possibility of breakup in the T-junction. Also, by enhancing the velocity of the continuous fluid, the probability of splitting of the mother microdroplet at micro T-junction rises. An increment in surface tension amongst the two phases without altering the initial length of the mother microdroplet causes a smaller probability of separation at the T-junction [23].

Also, using magnetic fields [30-36] and electrical fields [37] are other techniques that have been noticed recently in controlling of the splitting process of the mother microdroplets. By adding magnetic nanoparticles to different fluids, magnetic properties can be created, which can be controlled by a magnetic field [30, 32, 34-36, 38, 39]. This type of fluid, which has magnetic properties, is called ferrofluid. Ferrofluids have been utilized in many fields such as heat transfer enhancement [40], droplet formation [41-44], and manipulation [45]. One of the ways that can be used to cause asymmetric breakup at junctions is to create an asymmetric magnetic field at the center of the junction [23, 39, 46]. In this situation, the ferrofluid can be affected due to the magnetic force created by the magnetic field. To do this, a magnetic field can be placed under one of the T-junction branches. In this case, if the ferrofluid microdroplets, flow into the center of the T-junction, they will be affected by the asymmetric field due to magnetic properties and break asymmetrically at the end of the T-junction [23]. In these situations, the splitting ratio can be defined as "the volume of the microdroplet moves to the branch with less hydrodynamic resistance divided to the total volume of the mother microdroplet" [23].

$$Splitting\ Ratio = \frac{\text{Volume of droplet which goes to branch with less resistance}}{\text{Total Volume of mother microdroplet}} \quad (1)$$

where, 0.5 still means symmetric breakup and 1 means non-breakup. It is also possible to achieve a splitting ratio between 0.5 to 1 in these cases [23].

So, to reach asymmetric breakup of microdroplets, changing the surface tension among the discrete and continuous fluids [29] and utilizing various geometries [18, 26, 47] is suggested. Moreover, using magnetic force to breakup magnetic microdroplets and examination of flow regime is studied numerically and experimentally [39, 46, 48]. But, in earlier findings, the analysis of the impact of using asymmetric magnetic force in an asymmetric T-junction is not investigated yet. So, although many studies have been conducted in recent years on microdroplets' breakup, manipulating microdroplets' breakup in a T-junction with different branch widths in the presence of an asymmetric magnetic field has not been studied numerically. The purpose of the present paper is to study the microdroplets' breakup phenomenon in T-junctions with different branch widths under the influence of asymmetric magnetic field numerically for the first time. The main advantage of this technique is that it allows for easier control and fine-tuning of microdroplets' splitting ratio at T-shaped junctions.

2. Geometrical Specifications

The schematic layout of the geometry used to study the breakup phenomenon in microdroplets is depicted in Fig. 1. The setup is comprised of a two-dimensional T-junction with equal-length branches, with a magnetic field, created from a magnetic dipole, acting under the right branch. The field exerts a volumetric force to the ferrofluid inside the microchannel [14, 23]. In this state, a ferrofluid microdroplet (referred to as droplet for simplicity from here on out) made of ferrofluid in water base (discrete phase) which is driven by oil (continuous phase) enters the T-junction with constant velocity. The viscosity and the density of the continuous fluid that carried the droplets were 0.00125 (kg/(m.s)) and 800.0 kg/m^3, respectively. Also, the viscosity and the density of the droplets were 0.001 (kg/(m.s)) and 998.20 kg/m^3. The surface tension between the two fluids was assumed to be 0.005 N/m. The initial condition is shown in Fig. 1. As the droplet enters the junction, because of the magnetic field effect and the width ratio between the left and right branches, it might breakup in asymmetric ratios or pass unbroken through the branch above the magnetic field [23].

3. Governing Physics

A water-based ferrofluid droplet is considered inside the microchannel. The forces applied on this droplet are as follows [14, 18, 20, 23, 26]:

- Inertial force, which appears because of the continuous fluid motion.
- Surface tension force, which affects the droplet in motion and prevents its deformation.
- Magnetic force due to the existing field: For droplets which contain magnetic nanoparticles, a force is applied by the magnetic field beneath the right branch. This volumetric force is caused by the presence of a magnetic line dipole [14, 23]. Magnetic line dipole is a magnetic field constructed from two straight currents with opposite directions. For the simulations carried out in this study, different intensities have been considered for the magnetic dipole, which can generate different volumetric forces at the center of the junction. Therefore, ferrofluid droplets can be affected by different amounts of volumetric forces. The magnetic field in the desired range can be obtained as follows [14, 23]:

$$\vec{B} = \mu_0(1+\chi_m)m\left(\frac{\sin\alpha}{r^2}\vec{e}_r - \frac{\cos\alpha}{r^2}\vec{e}_\alpha\right); \qquad \text{for } r \gg b \tag{2}$$

In which $m = bI/2\pi$. m is the magnetic dipole moment per unit length, b is the distance between two straight currents with opposite directions and I refers to current intensity (A). μ_0 is free space permeability which is equal to $4\pi\times10^{-7}\,\text{N/A}^2$. χ_m is magnetic susceptibility, r is the distance from the dipole, $\vec{e_r}$ and $\vec{e_\alpha}$ are unit vectors and α is the polar angle. It should be noted that Eq. 2 is correct for the $r >> b$. In this study, two straight currents with opposite directions were used to generate the magnetic field [14]. In this case, the magnetic field source is called a line dipole. This magnetic field is proportional to $1/r^2$ and the dimension of m is A.m. In this paper, the ferrofluid susceptibility is assumed very low ($\chi_m = 0.06$) for ferrofluid with small magnetic nanoparticles concentrations and so, $H \approx H_0$ approximation is considered. However, this solution is only valid for ferrofluids with low susceptibilities and accurate results would be obtained if Navier-Stokes and Maxwell equations are solved simultaneously.

Mass and momentum equations are as follows [30]:

$$\frac{\partial\rho}{\partial t} + \vec{\nabla}.\left(\rho\vec{V}\right) = 0 \tag{3}$$

$$\frac{\partial\left(\rho\vec{V}\right)}{\partial t} + \vec{\nabla}.\left(\rho\vec{V}\vec{V}\right) = -\vec{\nabla}p + \vec{\nabla}.\vec{\tau} + \vec{f} \tag{4}$$

in which ρ is density (kg/m^3), t is time (s), $\vec{V}$ is velocity, p is pressure, $\vec{\tau}$ is viscous stress tensor and $\vec{f}$ is Kelvin's body force. The amount of $\vec{\nabla}.\vec{\tau}$ in momentum equation (Eq. 4) can be expressed as [24, 30]:

$$\vec{\nabla}.\vec{\tau} = \vec{F}_{\text{int}} + \mu\frac{\partial^2 \upsilon_j}{\partial x_j^{\,2}} \tag{5}$$

Hence, Eq. 4 can be written as [30]:

$$\rho\left(\frac{\partial \upsilon_i}{\partial t} + \upsilon_j\frac{\partial \upsilon_i}{\partial x_j}\right) = -\vec{\nabla}p + \vec{F}_{\text{int}} + \mu\frac{\partial^2 \upsilon_i}{\partial x_i \partial x_j} + \vec{f} \tag{6}$$

The effect of the surface tension force $\vec{F}_{\text{int}}$ is given by $F_i = \sigma\kappa\delta_s\hat{n}_i$ where σ represents the interfacial tension and κ stands for the mean curvature of the interface [24]. Also, δ_s and $\hat{n}_i$ depicts the delta function and the interface unit normal vector, respectively. The normal vector can be calculated for the cells near the wall using the following relation: where $\hat{n}_i = \hat{n}_w\cos\alpha + \hat{t}_w\sin\alpha$, $\hat{n}_w$ and $\hat{t}_w$ are the unit vectors normal and tangential to the wall surface, respectively. [24]

In Eq. 6, ρ and μ are considered as average viscosity and density for each computational cell, respectively. The values of these two properties can be calculated as [14, 23]:

$$\rho = \rho_c\phi + \rho_d(1-\phi) \tag{7}$$

$$\mu = \mu_c\phi + \mu_d(1-\phi) \tag{8}$$

In Eqs. 7 and 8, the c and d subscripts represent continuous and discrete phases. ϕ denotes the volumetric ratio of the continuous fluid in every grid. In all the computational cells, ϕ is between 0 (fully filled by the dispersed phase) and 1 (completely occupied by the continuous phase). ϕ is solved by the following equation [24]:

$$\frac{\partial \phi}{\partial t} + \upsilon_j \frac{\partial \phi}{\partial x_j} = 0 \tag{9}$$

If the volume fraction is not equivalent to its highest or lowest values (1 or 0), it implies that the cell is filled by both phases and the boundary of the dispersed phase (interface of ferrofluid droplet) is considered to be positioned with $\phi = 0.5$.

The last term $\vec{f}$ in Eq. 6, depicts the magnetic force which is the sum of volume and surface forces. The surface force is neglected because the magnetic susceptibility of ferrofluid is very low and the volumetric force and is expressed as follows [49, 50]:

$$\vec{f} = \mu_0 \vec{M} \nabla \vec{H} \tag{10}$$

$\vec{M}$ reflects the magnetization in Eq. 10. This term is the force that is imposed on the ferrofluid because of its existence in magnetic field [14, 23].

For smaller temperatures, the magnetic current magnitude vector $\vec{M}$ could be linked to $\vec{H}$ by [14, 23, 49]:

$$\vec{M} = \chi_m \vec{H} \tag{11}$$

In Eq. 11, $\vec{H}$ reflects the magnetic field strength (A/m). Also χ_m is assumed to be constant because low magnetic inductions are applied to the ferrofluid droplet. In this case, the operating condition falls within the low values of magnetic field strength and magnetization and so the slope of the curve (χ_m) can be assumed constant.

As presented before [18, 23, 26], in a symmetrical T-junction, there are two possibilities for the fate of an entering droplet. It can either break into two equal-size droplets or not breakup at all. For the first scenario, because the volumes of the daughter droplets are equal, the splitting ratio is 0.5 [23]. Based on the definition, the 0.5 splitting ratio indicates the symmetrical breakup of the droplet, while the splitting ratio of 1 is attributed to no breakup. However, if symmetry no longer holds, the splitting ratio will have a value between 0.5 to 1 [23]. In the current study, the symmetry in the T-junction is disrupted by having different widths for the two outlet branches ($WR = W_2 / W_1$) and existence of an asymmetric magnetic field which locates beneath of the wider branch (right branch). The magnetic force stemming from a dipole under the right branch makes a higher volume of ferrofluid droplet likely to enter the right branch. Also, due to the greater width of the right branch with respect to the left one, the hydrodynamic resistance of the right branch is lower than the left naturally, which further helps the asymmetric breakup of the droplet [18]. Hence, two events may occur for a ferrofluid droplet inside a T-junction with unequal branch widths under an asymmetric magnetic field [23]:

- The ferrofluid microdroplet exits from the right branch (which is less resistant due to greater width and the presence of a magnetic field) without breaking at the T-junction. In this case, according to the definition, the breakup ratio will be equal to 1.
- The ferrofluid droplet breaks inside the T-junction and creates two daughter droplets. In this case, the volume of the daughter droplets will definitely be different due to the asymmetry in the width of the branches and the asymmetric magnetic field. Therefore, according to the definition, the failure ratio in this numerical case will be between 0.5 to 1.

Time sequencing of non-breakup and breakup regimes is shown in Fig. 2(a) and (b), respectively.

4. Numerical Algorithm

The finite volume method in OpenFoam software was used to solve the problem. One of the conventional strategies to study and track the interface in a two-phase system (water-based ferrofluid as discrete fluid and oil as continuous fluid) in the finite volume method is the use of the volume of fluids (VOF) method [18, 20, 23].

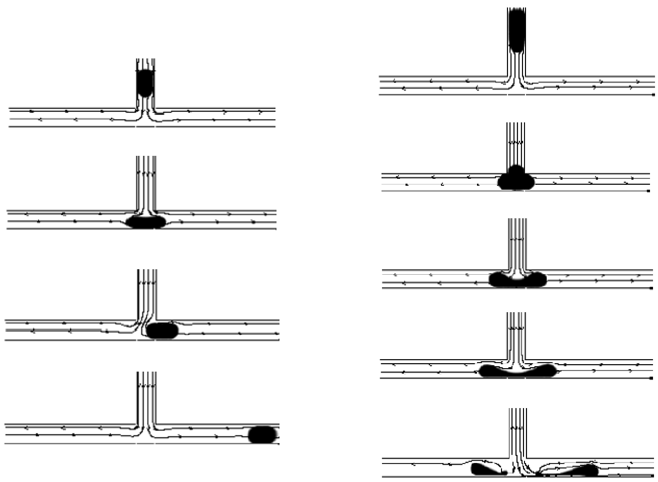

(a) (b)

Fig. 2. (a) breakup and (b) non-breakup regimes.

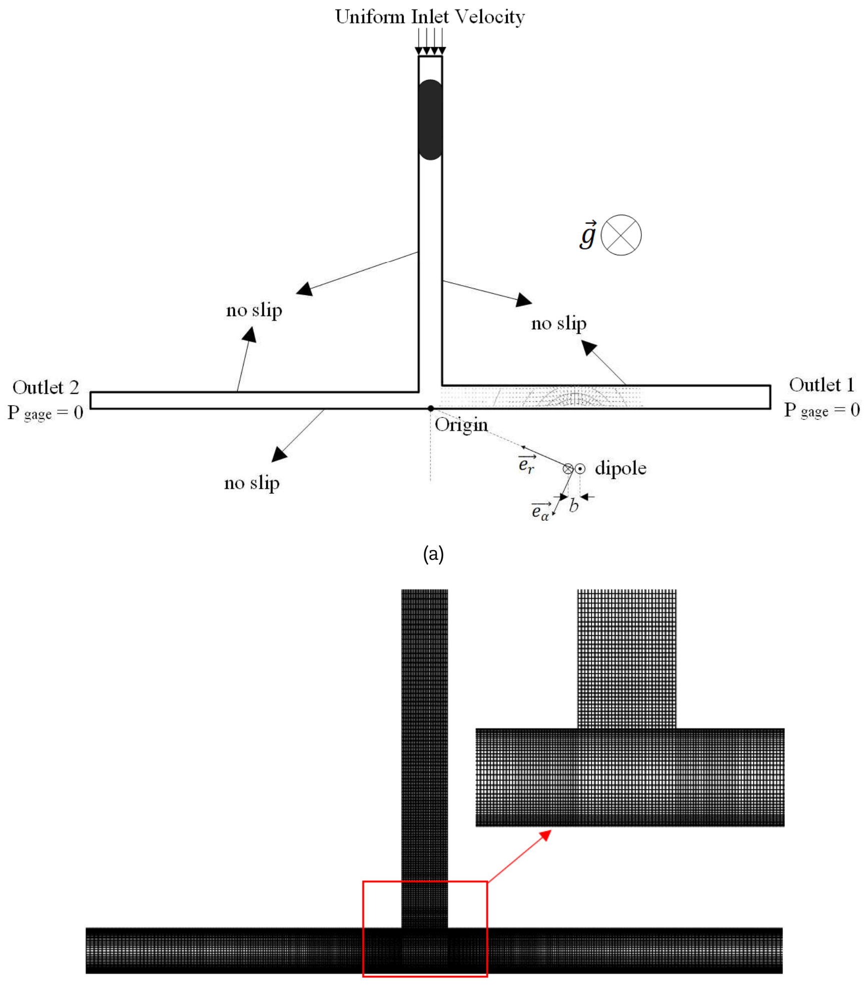

Fig. 3. (a) Boundary conditions used to solve the problem. Constant velocity at the inlet for the continuous fluid, no-slip boundary condition for the walls and zero gauge pressure for the outlets of the T-junction. (b) computational mesh utilized in this study.

In the current study, the phases are assumed to be incompressible and immiscible, and the problem is solved by considering suitable boundary conditions. The boundary conditions, as depicted in Fig. 3(a), include constant velocity at the inlet for the continuous fluid, the no-slip boundary condition for the walls and the pressure considered as zero gauges at the outlets of the branches. The computational mesh used in this study is shown in Fig. 3(b).

The variables are the velocity of the continuous fluid at the inlet, magnetic field density, and the widths of the left branch. The outlet pressures were held constant at all times. In the course of running the simulation in different states, two ferrofluid droplets with non-dimensional lengths of 1.77 and 2.77 were used to allow for a better analysis. The non-dimensional length is defined as L / W_1 ratio with L as the initial length of the droplet at the inlet of the microchannel and W_1 as the width of the main branch of the microchannel. In order to evaluate the results in different states, the non-dimensional ratio of the widths ($WR = W_2 / W_1$) was used, in which as stated before, W_1 and W_2 are the widths of the right and left branches, respectively (for this problem, as it can be seen in Fig. 1, the width of the main branch of the microchannel is 400 micron). The non-dimensional widths (WR) were 1, 0.85 and 0.7. The inlet velocity was changed by having different Capillary numbers (Ca), which is the ratio of continuous fluid inertia to surface tension ($Ca = \mu_c V_c / \sigma$). The Ca numbers used here were 0.03, 0.04, and 0.05. The magnetic field direction was altered using the Magnetic Bond number ($Magnetic\,Bo = \mu_0 W_1 H^2 / \sigma$), in which μ_0 is the magnetic permeability coefficient in vacuum with a value of $4\pi \times 10^{-7} N / A^2$ and $\vec{H}$ is magnetic field strength vector (A/m). The Magnetic Bond number range was from 0 (no magnetic field) to 104. It should be noted that although the diagrams are expressed in terms of magnetic Bond number, the process of ferrofluid droplet splitting depends on both the magnitude and direction of applied magnetic force. In this study the position of the magnetic dipole is kept fixed and so it can be extrapolated for different magnetic Bond numbers in the problems that uses a magnetic dipole in the same position. However, for different positions of the magnetic dipole, the results are qualitatively valid (e.g., the splitting ratio increases with an increasing in magnetic Bond number if a dipole is placed anywhere on the right-hand side). The mesh and time step intendancy of the numerical results were checked. For this purpose, each geometry has meshed with 10024, 20058, 30078, 40102, and 50112 elements, and the obtained results to determine the splitting ratio of the droplet had a difference of less than 1% in the 30078-node grid compared to the finest grid.

Time independency is also examined. The results revealed that a time step of 2×10^{-6} is appropriate for the transient simulations. The QUICK scheme is utilized for the discretization of the momentum equation, and the SIMPLEC scheme is utilized for the pressure-velocity coupling.

Table 1. Grid independency study (L/W_1=1.77, Ca=0.04, WR=0.85 and Magnetic Bond=58.5)

Grid Number	Splitting ratio (S.R)	$\frac{S.R^{i+1} - S.R^{i}}{S.R^{i+1}}$
10024	0.6123	0.116
20058	0.6928	0.044
30078	0.7249	0.003
40102	0.7276	0.001
50112	0.7288	-

Table 2. Verification for m = 0

	m	V_0	Re	θ_b	$\overline{Nu}$
Reference [14]	0	0.005	11.8	0.59	2.61
Current simulations	0	0.005	11.8	0.5772	2.6541

5. Verification

In this section, at first, the results are verified. The results of droplet breakup in symmetric T-junctions are verified with the results of Leshansky and Pismen [15]. Afterward, the correctness of the magnetic force has been investigated.

It is necessary to introduce the concept of two parameters of L and L_c in order to validate the results. L is the initial length of the mother droplet at the starting of the process, while the critical length L_c depicts the maximum length of the mother droplet prior to its breakup in the T-junction [15].

Leshansky and Pismen [15] explained an analytical relationship which can define a curve amongst non- breakup and breakup regions. The recommended equation is a function of the Ca number and can be defined by:

$$\frac{L_c}{w} = 1.3Ca^{-0.21} \tag{12}$$

where L_c is the mother droplet length just before breakup in the T-junction and W is the channel width. To verify the accuracy of the numerical method, the simulation results for the Ca number and the non-dimensional length ratio of the droplet in the T-junction without magnetic field were validated with the analytical results of Leshansky and Pismen [15] as can be seen in Fig. 4.

Based on Fig. 4, it is observed that the present results are precisely predicted the borderline between separating and non-separating regions in the T-junction and is in agreement with the results of Leshansky and Pismen [15].

Furthermore, to evaluate the impact of the magnetic field on the ferrofluid material, a water-based ferrofluid flow, both in the existence and absence of external magnetic force with the same boundary conditions as in Ref. [14] were utilized to perform computations. This article is utilized for the second part of verification, because a line dipole was chosen to apply the magnetic field, which is related to the methodology applied in the present study. The line dipole is placed at x/h=5. First, in case (a), Nusselt number ($\overline{Nu} = (\int Nudx\,, x = 0 \text{ to } l)/l,\;\; Nu = q''_w C/(k(T_h - T_f))$) where l is the length of the plate, q''_w denotes wall heat flux, C is convection heat transfer coefficient, k is thermal conductivity and T denotes temperature) and dimensionless exit flow temperature ($\theta_b = (T_b - T_f)/(T_h - T_f)$, where b, f, and h are pertaining to the temperatures of bulk fluid, cold wall, and heated inlet) were computed in the absence of the magnetic field. Table 2, indicates that the deviations among the present results and those of Ref.[14] for Nu and θ_b are 1.69%, and 2.17%, respectively.

Velocity vectors and temperature contours, demonstrated in Figs. 5, show an excellent agreement amongst previous studies and current computations.

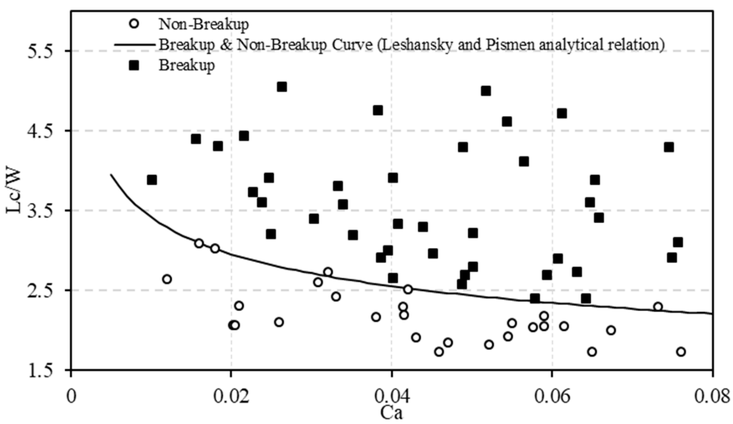

Fig. 4. Comparison of results of the current model (spots and squares) and the analytical relation of Leshansky and Pismen (the curve which is described as $L_c/w = 1.3Ca^{-0.21}$). The borderline describes the analytical relation which determines the breakup & non-breakup region in Leshansky and Pismen work while the spots and squares describe the situations of different microdroplets with different Ca numbers obtained in this paper.

Table 3. Verification for $m = 0.19 \times 10^{-4}$ $A.m$

	m	V_0	Re	θ_b	$\overline{Nu}$
Reference [14]	1.90E-05	0.005	11.8	0.58	2.67
Current Solution	1.90E-05	0.005	11.8	0.5725	2.688

The simulations were further evaluated alongside the case (b) of Ref. [14] in Table 3. In the existence of a magnetic field, the results show a discrepancy of 0.67% for the Nusselt number and 1.29% for θ_b , that shows a good agreement amongst the results of the present work and those of the Ref.[14]. The temperature contours for the present analysis are presented in Figs. 6. The effects of the dipole located in the middle of the channel are noticeable.

6. Results and Discussion

Figs. 7(a) to 7(c) show the variations of the splitting ratio of ferrofluid droplets against Magnetic Bond number at a constant non-dimensional length of 1.77 for different *Ca* numbers of 0.03, 0.04 and 0.05 and for three different width ratios (WR=0.7, 0.85 and 1).

It is shown that, the increment in Magnetic Bond number, enhances the splitting ratio before reaching 1. The physical explanation for this behavior lies in the fact that for any ferrofluid droplet at a constant *Ca* and width ratio, the greater the magnetic field intensity at the center of the junction, the greater the volume of the ferrofluid droplet will tend to enter the right branch.

There is an interesting point in Fig. 7(a). In this figure, the splitting ratio is equal to 1 for all the width ratios and Magnetic Bond numbers. As a matter of fact, the amount of *Ca* number is not enough for droplet splitting. It is depicted that the ferrofluid droplet passes through the T-junction without breakup in WR=1 and Magnetic Bond=0. Therefore, applying a magnetic field or making a change in the ratio of width branches does not change this splitting ratio.

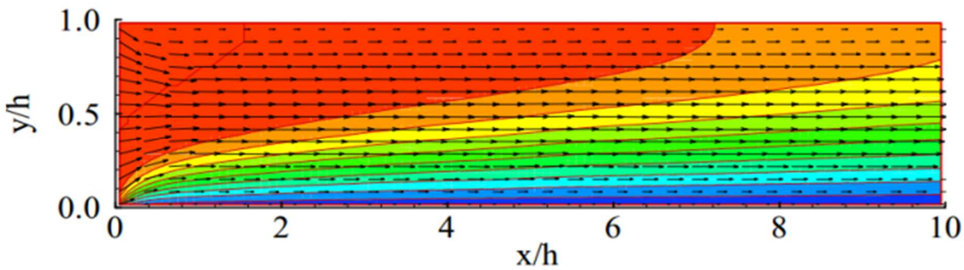

(a)

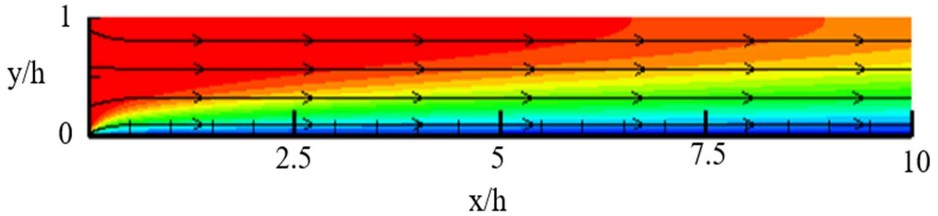

(b)

Fig. 5. Temperature Contour and velocity vector for $m = 0$ (a) Reference [14] (b) current simulation

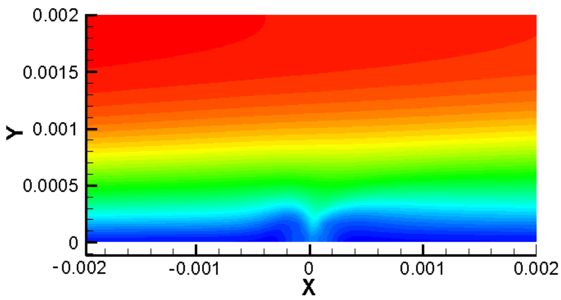

Fig. 6. Temperature Contour for $m = 0.19 \times 10^{-4}$ $A.m$, $\mathrm{Re} = 11.8$.

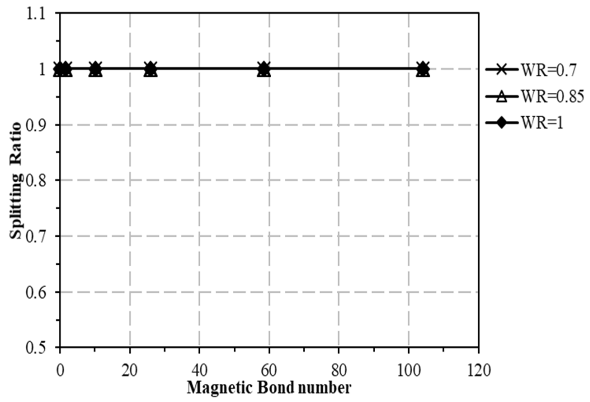

(a)

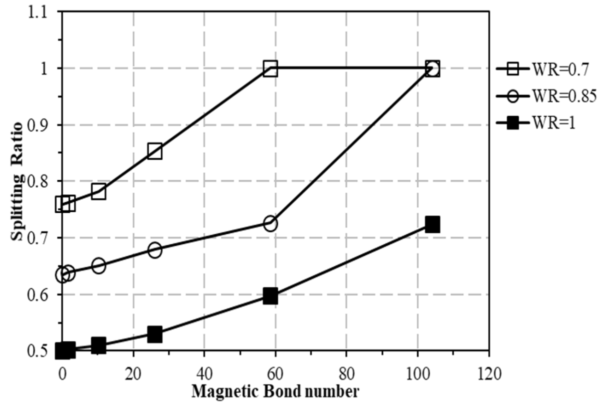

(b)

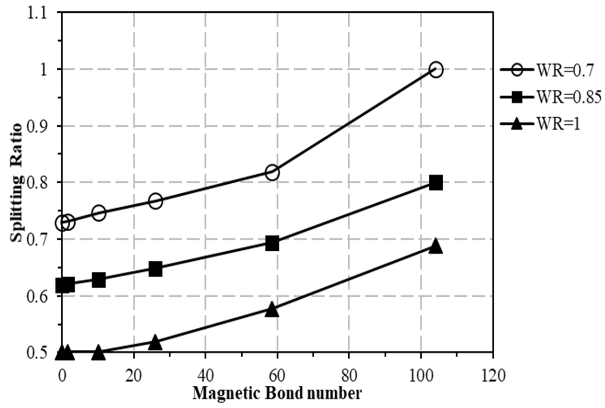

(c)

Fig. 7. Variations in splitting ratio vs. Magnetic Bond for L/W_1=1.77 and (a) *Ca*=0.03, (b) *Ca*=0.04, and (c) *Ca*=0.05 at three different width ratios.

Fig. 7(b) shows that by increasing the *Ca* number up to 0.04, the variation of splitting ratio against the Magnetic Bond number is ascending until it reaches 1. When the splitting ratio becomes 1, it indicates that the entire volume of the ferrofluid droplet enters the right branch. It is seen in this state that with increasing magnetic field intensity, no change will occur to the splitting ratio because the entire volume of the ferrofluid droplet enters the right branch. For instance, in Fig. 7(b) at *Ca*=0.04, WR=1 and non-dimensional length of 1.77, when Magnetic Bond number is zero, the breakup will be symmetrical (splitting ratio = 0.5); but as the Magnetic Bond number increases, the splitting ratio increases up to 1. By further increasing in Magnetic Bond number, the splitting ratio remains constant at 1. It should be noted that the greater the magnetic force at the center of the junction, the greater the ability of the ferrofluid droplet to move toward the right branch. In fact, a larger volume of the ferrofluid droplet will tend to enter the right branch due to the presence of a stronger volumetric magnetic force.

The other noteworthy point is the effect of WR on ferrofluid droplet breakup. As seen in Figs. 7(b) and (c), for a specific ferrofluid droplet at constant *Ca* and Magnetic Bond number, by decreasing the width ratio (more asymmetrical T-junction) the splitting ratio increases. Fig. 7(c) shows that just by changing WR (geometrical asymmetry), the splitting ratio at the Magnetic Bond of 0 is 0.5 for WR=1, 0.62 for WR=0.85, and 0.73 for WR=0.7. This illustrates that without applying the magnetic force at the center of the junction, it is possible to achieve arbitrary splitting ratios only by altering the branch width ratio (WR). Therefore, the change in branch width ratio, as well as the change in magnetic field intensity can be effective in controlling the breakup ratio. Also, it can be seen that in Fig. 7(c), the splitting ratio at *Magnetic Bo*=58.5 and WR=1 is 0.58. On the other hand, this number is 0.7 and 0.83 for width ratios of 0.85 and 0.7 at the same Magnetic Bond number. This means that the variations in the width ratio of the T-junction significantly reduces the hydrodynamic resistance of the right branch, allowing a higher volume of ferrofluid droplets to enter the right branch. In other words, by altering the width ratio of the branches in a T-junction and the hydrodynamic resistance of the branches along with changing the Magnetic Bond number, there is a higher control on the breakup of ferrofluid droplets to reach the desired splitting ratio.

Similarly, the splitting ratio against the Magnetic Bond number for L/W_1=2.77 is depicted in Fig. 8(a) to (c).

The main behavior as Fig. 7 can be seen in Fig. 8, but a slight difference exists. By increasing the non-dimensional lengths, the splitting ratio decreases at the same conditions. For instance, the splitting ratio in Fig. 8(a) covers a wide range between 0.5 and 1, whereas all the splitting ratios in Fig. 7(a) are one.

Figs. 9(a) to 9(c) show the variations in splitting ratio against Magnetic Bond number at L/W_1=1.77 in different *Ca* numbers for WR=1, 0.85, and 0.7, respectively.

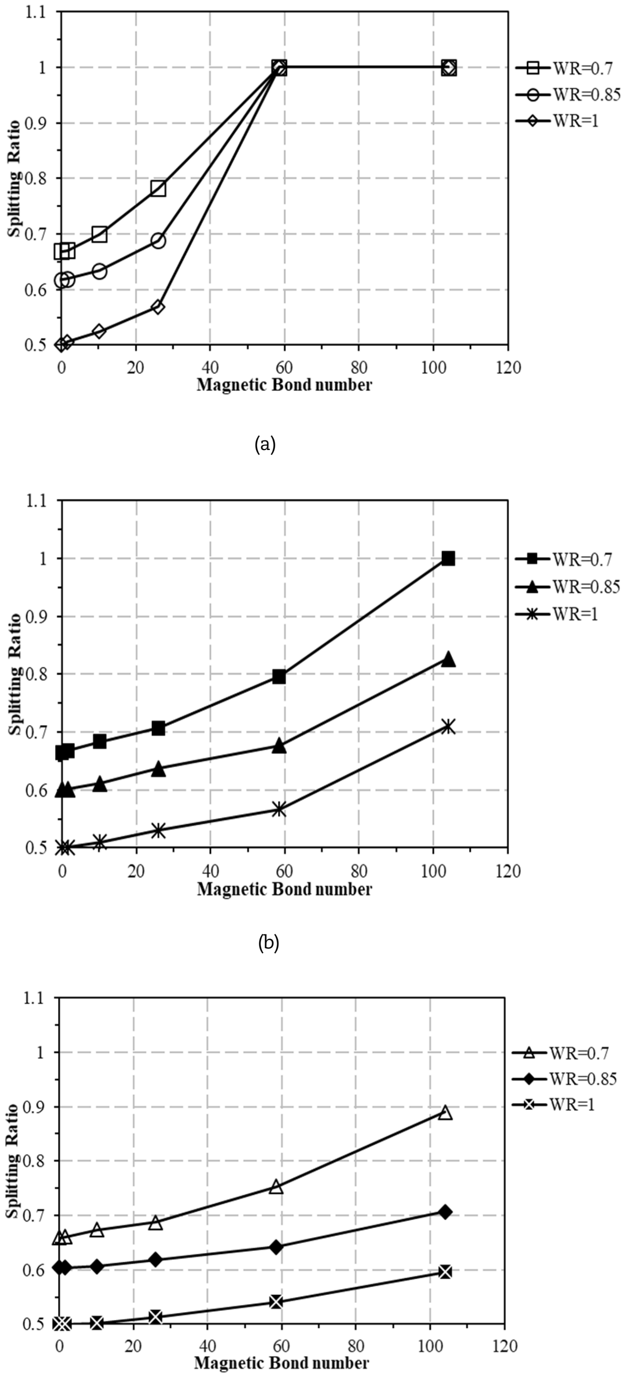

(a)

(b)

(c)

Fig. 8. Variations in splitting ratio vs. Magnetic Bond for L/W_1=2.77 and (a) *Ca*=0.03, (b) *Ca*=0.04, and (c) *Ca*=0.05 at three different width ratios.

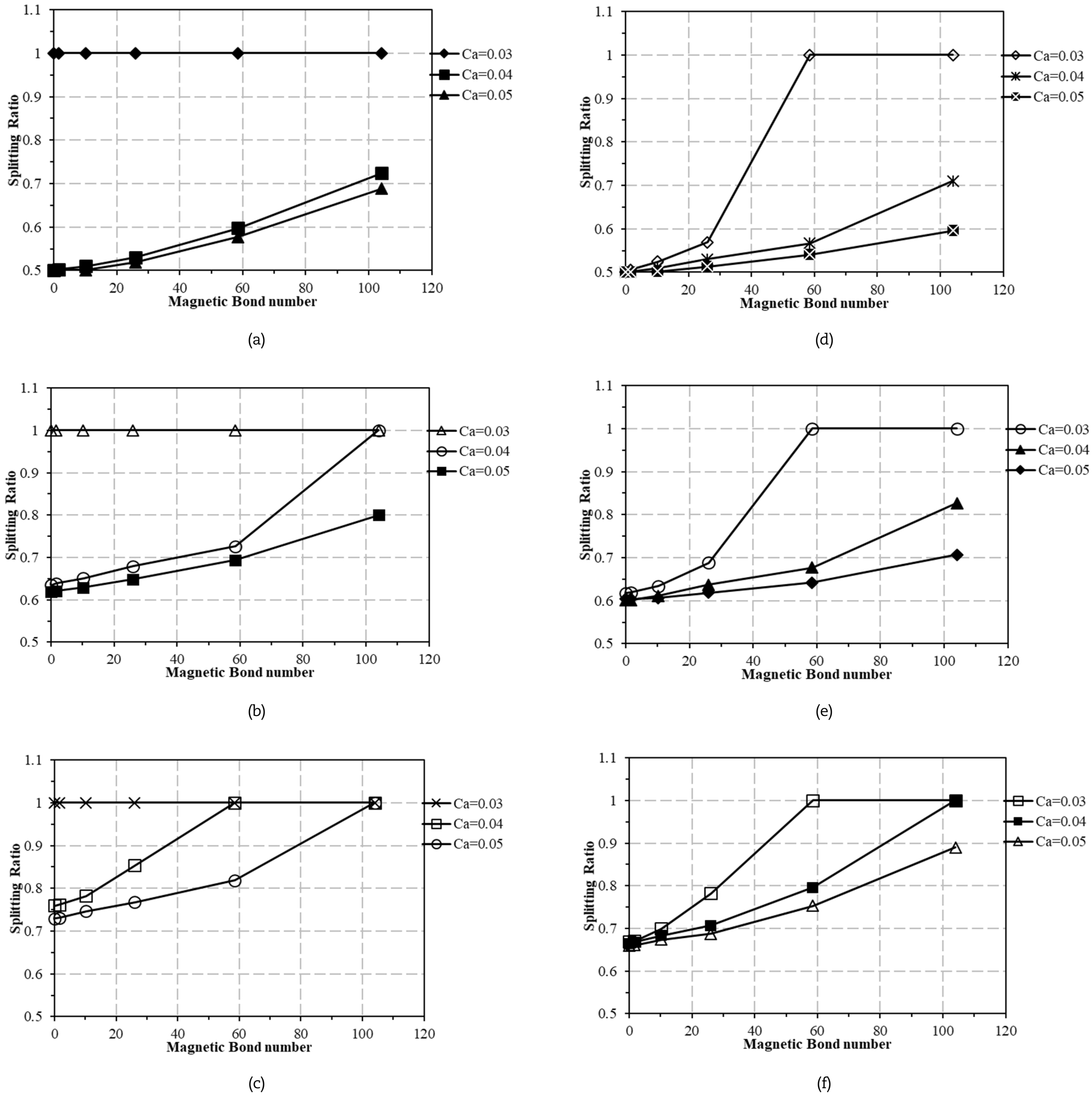

Fig. 9. The variations of splitting ratio against Magnetic Bond number for various *Ca* numbers and constant (a) WR=1, and L/W_1=1.77, (b) WR=0.85, and L/W_1=1.77, (c) WR=0.7, and L/W_1=1.77, (d) WR=1, and L/W_1=2.77, (e) WR=0.85, and L/W_1=2.77, (f) WR=0.7, and L/W_1=2.77.

As illustrated in these figures, the *Ca* number plays an important role in the droplet breakup process. Generally, as the *Ca* number increases the splitting ratio decreases at a constant Magnetic Bond number. For instance, as seen in Fig. 9(b), for low *Ca* number (0.03) splitting ratio is equal to 1 for all Magnetic Bond numbers. This indicates that the inertial force is very low relative to a magnetic force that it does not breakup in the junction and its entire volume enters the right branch. However, by increasing the Ca number, the magnetic force could not pull the entire volume of the ferrofluid droplet to the right branch and the droplet would breakup. It can be seen that at a constant Magnetic Bond number of 58.5, by increasing *Ca* from 0.03 to 0.04, the splitting ratio decreases from 1 to 0.73. In fact, the effect of *Ca* number and Magnetic Bond number on splitting ratio is reverse; increasing the *Ca* number in a constant condition yields to decrease in splitting ratio, whereas by increasing the Magnetic Bond number considering the fixed situation, the droplet splitting enhances. Also, by increasing the width ratio from Figs. 9(a) to 9(c), the same trend is observed, while more asymmetric droplet splitting could be achieved.

Similarly, the splitting ratio behavior is shown in Figs. 9(d) to 9(f) for L/W_1=2.77 in different *Ca* numbers for WR=1, 0.85, and 0.7, respectively. It is depicted that in these figures the general trend is the same as that of L/W_1=1.77. For example, in Fig. 9(e) by increasing the *Ca* number from 0.03 to 0.05 at a constant Magnetic Bond number equal to 58.5, the splitting ratio decreases from 1 to 0.68 and then reduce to 0.65.

Figs. 10(a) to (c) show the variation of the splitting ratio with Magnetic Bond number for the two ferrofluid droplets of varying non-dimensional lengths of 1.77 and 2.77.

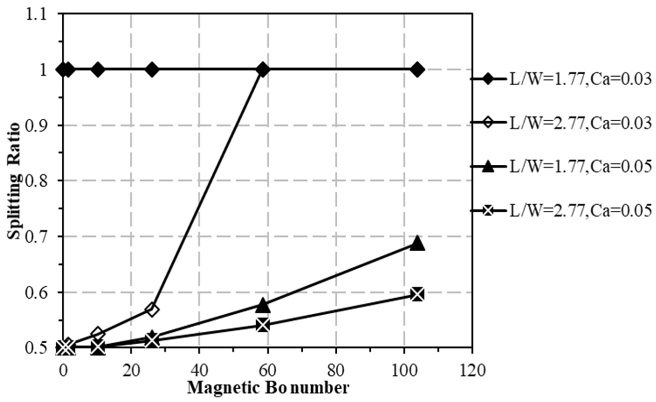

(a)

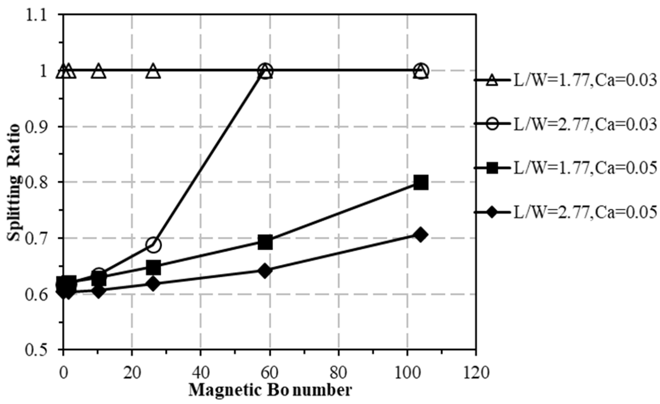

(b)

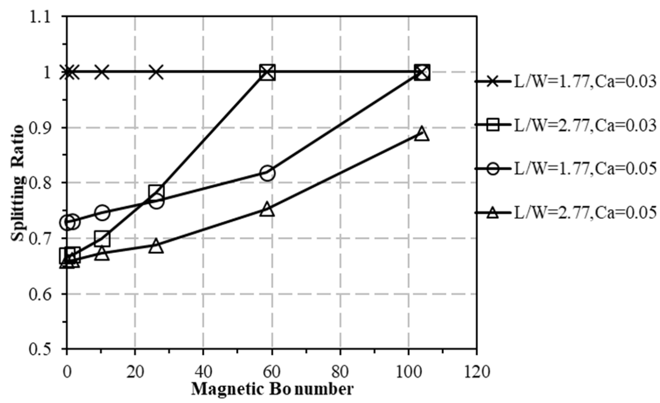

(c)

Fig. 10. Variations in splitting ratio vs. Magnetic Bond number for comparing L/W_1=1.77 and 2.77 and (a) WR=1, (b) WR=0.85, and (c) WR=0.7 at different *Ca* number.

In each diagram of Fig. 10(a) to 10(c), two different *Ca* numbers are considered. The general trend in Fig. 10 is that the splitting ratio increases with increment in Magnetic Bond number. The important point in these graphs is that if the splitting ratio of two non-dimensional ferrofluid droplets for a fixed WR, *Ca* and a Magnetic Bond number are compared, the smaller ferrofluid droplet has a higher splitting ratio or equals the larger ferrofluid droplet. When the splitting ratio is equal for both small and large ferrofluid droplets, the non-breakup state occurs for both of the ferrofluid droplets under simulated conditions. In fact, the splitting ratio of the larger ferrofluid droplet is always smaller than the splitting ratio of the smaller ferrofluid droplet unless the larger ferrofluid droplet does not breakup within the T-junction, where the splitting ratio will be equal to 1. It seems that if the larger ferrofluidic droplet does not break through the T-junction under simulated conditions, the smaller ferrofluidic droplet will not break either. The physical reason for this phenomenon can be interpreted as, under the same conditions of the simulation, the asymmetric magnetic field intensity is able to affect the larger percentage of the volume of the smaller ferrofluid droplet, and thus the greater the percentage of the ferrofluid droplet volume goes to the right branch.

7. Conclusion

In this study, the variation of splitting ratios for ferrofluid droplets within a T- junction with different branch widths in the presence of an asymmetric magnetic field is investigated. The effect of four dimensionless parameters including, the width ratio of the T-junction, Magnetic Bond number, Capillary number, and the non-dimensional droplet length on the splitting ratio is studied. The splitting ratio varies between 0.5 and one. For a ferrofluid droplet in a symmetrical T-junction (WR=1), if there is no magnetic field in the system (Magnetic Bond=0), then the splitting ratio would be only 0.5 or 1. That is, the mother droplet either splits into two smaller droplets with equal volumes and each new droplet passes through one branch (splitting ratio=0.5) or it passes without breaking through the branch with lower resistance (splitting ratio=1). In this case, the branch with lower resistance is determined by numerical calculations. So, when a numerical simulation is carried out, in order to go from one time step to the next, some calculations should be rounded up for computational cells. As a result, the round-up changes the hydrodynamic resistance of the branches and directs the drop toward the branch with less resistance. For a given ferrofluid droplet in a T-junction, as the width ratio increases, the splitting ratio decreases. Also the greater the Magnetic Bond number, the greater the ferrofluid droplet volume tends to enter the right branch due to the presence of the magnetic field beneath the right branch of the T-junction, and so the splitting ratio increases. On the other hand, an increase in the Capillary number results in a reduction in the splitting ratio. Also, an increment in non-dimensional droplet length leads to a reduction in splitting ratio. Therefore, this investigation shows that to control the ferrofluid droplets breakup and reaching various splitting ratios, simultaneous use of a T-junction with different width ratios and an asymmetric magnetic force are recommended.

Author Contributions

M. Aboutalebi initiated the project, validated the results, conducted the simulations, and wrote the original manuscript; M.B. Shafii planned the scheme, suggested the simulations, and edited the manuscript; S.K. Hannani edited and reviewed the manuscript. The manuscript was written through the contribution of all authors. All authors discussed the results, reviewed, and approved the final version of the manuscript.

Acknowledgments

We would like to express our gratitude to the Deputy of Research and Technology of Sharif University of Technology and Sharif Energy Research Institute (SERI) for providing a comfortable working environment to carry out experiments.

Conflict of Interest

The authors declared no potential conflicts of interest with respect to the research, authorship, and publication of this article.

Funding

The authors received no financial support for the research, authorship, and publication of this article.

Data Availability Statements

The datasets generated and/or analyzed during the current study are available from the corresponding author on reasonable request.

Nomenclature

b	Distance between the conductors (m)	$\hat{t}_w$	The unit vectors tangential to the wall surface
$\vec{B}$	Magnetic flux density (T)	$\vec{V}$	Velocity (m/s)
C	Convection heat transfer coefficient (W/m^2.K)	W_1	Width of the main branch and the right branch of the microchannel (400 µm)
Ca	Capillary number	W_2	Width of the left branch of the microchannel (µm)
$\vec{e_r}$	Unit vector	WR	Width ratio (L/W_1)
$\vec{f}$	Magnetic force applied on the ferrofluid droplet (N)	x	Axial distance (m)
$\vec{F}_{\text{int}}$	Surface tension force (N)	y	Height (m)
$\vec{H}$	Magnetic field strength (A/m)	***Greek symbols***	
h	Channel height (m)	α	Polar angle
I	Current (A)	δ_s	Kronecker delta
k	Thermal conductivity (W/m.K)	θ_b	Non-dimensional temperature
l	Length of the plate (m)	κ	Mean curvature of the interface
L	Initial length of the ferrofluid droplet (m)	μ	Dynamic viscosity (Pa s)
L_c	Maximum length of the ferrofluid roplet during passing the center of T junction (m)	μ_0	Magnetic permeability coefficient in vacuum (N/A^2)
$\vec{M}$	Magnetization (A/m)	ρ	Density (kg/m^3)
m	Dipole moment of line dipole per unit length (A.m)	σ	Surface tension between two fluids (N/m)
Magnetic Bo	Magnetic Bond number	$\vec{\tau}$	Viscous stress tensor (Pa s)
Nu	Local Nusselt number	ϕ	Volumetric ratio of the continuous fluid in each computational cell
$\overline{Nu}$	Average Nusselt number	χ_m	Magnetic susceptibility

$\hat{n}_i$	Unit vectors to the wall surface		***Subscripts***	
$\hat{n}_w$	Unit vectors normal to the wall surface		b	Bulk fluid
p	Pressure (Pa)		c	Continuous-phase
q_w''	Wall heat flux (W/m^2)		d	Discrete-phase
r	Radius (m)		f	Cold wall
Re	Reynolds number		h	Heated inlet
S.R.	Splitting ratio		w	Wall
T	Absolute temperature (K)			
t	Time (s)			

References

[1] T. Schneider, J. Kreutz, D.T. Chiu, The potential impact of droplet microfluidics in biology, *Analytical Chemistry*, 85(7) (2013) 3476-3482.

[2] D.J. Beebe, G.A. Mensing, G.M. Walker, Physics and applications of microfluidics in biology, *Annual Review of Biomedical Engineering*, 4(1) (2002) 261-286.

[3] S. Marre, K.F. Jensen, Synthesis of micro and nanostructures in microfluidic systems, *Chemical Society Reviews*, 39(3) (2010) 1183-1202.

[4] A. Shamloo, P. Vatankhah, M.A. Bijarchi, Numerical optimization and inverse study of a microfluidic device for blood plasma separation, *European Journal of Mechanics-B/Fluids*, 57 (2016) 31-39.

[5] Z.Z. Chong, S.H. Tan, A.M. Gañán-Calvo, S.B. Tor, N.H. Loh, N.-T. Nguyen, Active droplet generation in microfluidics, *Lab on a Chip*, 16(1) (2016) 35-58.

[6] P. Zhu, L. Wang, Passive and active droplet generation with microfluidics: a review, *Lab on a Chip*, 17(1) (2017) 34-75.

[7] L.-H. Chien, Y.-T. Cheng, Y.-L. Lai, W.-M. Yan, M. Ghalambaz, Experimental and numerical study on convective boiling in a staggered array of micro pin-fin microgap, *International Journal of Heat and Mass Transfer*, 149 (2020) 119203.

[8] L.-H. Chien, W.-R. Liao, M. Ghalambaz, W.-M. Yan, Experimental study on convective boiling flow and heat transfer in a microgap enhanced with a staggered arrangement of nucleated micro-pin-fins, *International Journal of Heat and Mass Transfer*, 144 (2019) 118653.

[9] C. Ho, Y.-C. Liu, M. Ghalambaz, W.-M. Yan, Forced convection heat transfer of Nano-Encapsulated Phase Change Material (NEPCM) suspension in a mini-channel heatsink, *International Journal of Heat and Mass Transfer*, 155 (2020) 119858.

[10] C.-Y. Chen, C.-H. Chen, L.-W. Lo, Breakup and separation of micromagnetic droplets in a perpendicular field, *Journal of Magnetism and Magnetic Materials*, 310(2) (2007) 2832-2834.

[11] M.A. Gijs, F. Lacharme, U. Lehmann, Microfluidic applications of magnetic particles for biological analysis and catalysis, *Chemical Reviews*, 110(3) (2009) 1518-1563.

[12] A. Ray, V. Varma, P. Jayaneel, N. Sudharsan, Z. Wang, R. Ramanujan, On demand manipulation of ferrofluid droplets by magnetic fields, *Sensors and Actuators B: Chemical*, 242 (2017) 760-768.

[13] H. Song, D.L. Chen, R.F. Ismagilov, Reactions in droplets in microfluidic channels, *Angewandte Chemie International Edition*, 45(44) (2006) 7336-7356.

[14] R. Ganguly, S. Sen, I.K. Puri, Heat transfer augmentation using a magnetic fluid under the influence of a line dipole, *Journal of Magnetism and Magnetic Materials*, 271(1) (2004) 63-73.

[15] A. Leshansky, L. Pismen, Breakup of drops in a microfluidic T junction, *Physics of Fluids*, 21(2) (2009) 023303.

[16] M.-C. Jullien, M.-J.T.M. Ching, C. Cohen, L. Menetrier, P. Tabeling, Droplet breakup in microfluidic T-junctions at small capillary numbers, *Physics of Fluids*, 21(7) (2009) 072001.

[17] A. Leshansky, S. Afkhami, M.-C. Jullien, P. Tabeling, Obstructed breakup of slender drops in a microfluidic T junction, *Physical Review Letters*, 108(26) (2012) 264502.

[18] A. Bedram, A. Moosavi, Droplet breakup in an asymmetric microfluidic T junction, *The European Physical Journal E*, 34(8) (2011) 1-8.

[19] M. Belloul, L. Courbin, P. Panizza, Droplet traffic regulated by collisions in microfluidic networks, *Soft Matter*, 7(19) (2011) 9453-9458.

[20] A. Bedram, A. Moosavi, Numerical investigation of droplets breakup in a microfluidic T-junction, in*: Applied Mechanics and Materials, Trans Tech Publ*, 2012, pp. 3269-3277.

[21] L. Salkin, A. Schmit, L. Courbin, P. Panizza, Passive breakups of isolated drops and one-dimensional assemblies of drops in microfluidic geometries: experiments and models, *Lab on a Chip*, 13(15) (2013) 3022-3032.

[22] U. Sen, S. Chatterjee, S. Sen, M.K. Tiwari, A. Mukhopadhyay, R. Ganguly, Dynamics of magnetic modulation of ferrofluid droplets for digital microfluidic applications, *Journal of Magnetism and Magnetic Materials*, 421 (2017) 165-176.

[23] M. Aboutalebi, M.A. Bijarchi, M.B. Shafii, S.K. Hannani, Numerical investigation on splitting of ferrofluid microdroplets in T-junctions using an asymmetric magnetic field with proposed correlation, *Journal of Magnetism and Magnetic Materials*, 447 (2018) 139-149.

[24] A. Bedram, A.E. Darabi, A. Moosavi, S.K. Hannani, Numerical investigation of an efficient method (T-junction with valve) for producing unequal-sized droplets in micro-and nano-fluidic systems, *Journal of Fluids Engineering*, 137(3) (2015) 031202.

[25] L. Ménétrier-Deremble, P. Tabeling, Droplet breakup in microfluidic junctions of arbitrary angles, *Physical Review E*, 74(3) (2006) 035303.

[26] M. Samie, A. Salari, M.B. Shafii, Breakup of microdroplets in asymmetric T junctions, *Physical Review E*, 87(5) (2013) 053003.

[27] Y. Fu, L. Bai, Y. Jin, Y. Cheng, Theoretical analysis and simulation of obstructed breakup of micro-droplet in T-junction under an asymmetric pressure difference, *Physics of Fluids*, 29(3) (2017) 032003.

[28] M. Yamada, S. Doi, H. Maenaka, M. Yasuda, M. Seki, Hydrodynamic control of droplet division in bifurcating microchannel and its application to particle synthesis, *Journal of Colloid and Interface Science*, 321(2) (2008) 401-407.

[29] P.-C. Hoa, Y.-F. Yap, N.-T. Nguyen, J. Chee-Kiong Chai, Thermally mediated droplet formation at a microfluidic T-junction, *Micro and Nanosystems*, 3(1) (2011) 65-75.

[30] J. Liu, S.-H. Tan, Y.F. Yap, M.Y. Ng, N.-T. Nguyen, Numerical and experimental investigations of the formation process of ferrofluid droplets, *Microfluidics and Nanofluidics*, 11(2) (2011) 177-187.

[31] S.-H. Tan, N.-T. Nguyen, L. Yobas, T.G. Kang, Formation and manipulation of ferrofluid droplets at a microfluidic T-junction, *Journal of Micromechanics and Microengineering*, 20(4) (2010) 045004.

[32] Y. Wu, T. Fu, C. Zhu, Y. Ma, H.Z. Li, Bubble coalescence at a microfluidic T-junction convergence: from colliding to squeezing, *Microfluidics and Nanofluidics*, 16(1-2) (2014) 275-286.

[33] N.-T. Nguyen, G. Zhu, Y.-C. Chua, V.-N. Phan, S.-H. Tan, Magnetowetting and sliding motion of a sessile ferrofluid droplet in the presence of a permanent magnet, *Langmuir*, 26(15) (2010) 12553-12559.

[34] X. Li, Z.-Q. Dong, P. Yu, X.-D. Niu, L.-P. Wang, D.-C. Li, H. Yamaguchi, Numerical investigation of magnetic multiphase flows by the fractional-step-based multiphase lattice Boltzmann method, *Physics of Fluids*, 32(8) (2020) 083309.

[35] X. Li, P. Yu, X.-D. Niu, D.-C. Li, H. Yamaguchi, A magnetic field coupling lattice Boltzmann model and its application on the merging process of multiple-ferrofluid-droplet system, *Applied Mathematics and Computation*, 393 (2021) 125769.

[36] C. Mu-Feng, L. Xiang, N. Xiao-Dong, L. You, Adnan, H. Yamaguchi, Sedimentation of two non-magnetic particles in magnetic fluid, *Acta Physica Sinica*, 66(16) (2017).

[37] J.S. Raut, S. Akella, A. Singh, V.M. Naik, Catastrophic drop breakup in electric field, *Langmuir*, 25(9) (2009) 4829-4834.

[38] S. Afkhami, A. Tyler, Y. Renardy, M. Renardy, T.S. Pierre, R. Woodward, J. Riffle, Deformation of a hydrophobic ferrofluid droplet suspended in a viscous medium under uniform magnetic fields, *Journal of Fluid Mechanics*, 663 (2010) 358-384.

[39] Y. Wu, T. Fu, Y. Ma, H.Z. Li, Active control of ferrofluid droplet breakup dynamics in a microfluidic T-junction, *Microfluidics and Nanofluidics*, 18(1) (2015) 19-27.

[40] M. Zarei Saleh Abad, M. Ebrahimi-Dehshali, M.A. Bijarchi, M.B. Shafii, A. Moosavi, Visualization of pool boiling heat transfer of magnetic nanofluid, *Heat Transfer—Asian Research*, 48(7) (2019) 2700-2713.
[41] M.A. Bijarchi, M.B. Shafii, Experimental investigation on the dynamics of on-demand ferrofluid drop formation under a pulse-width-modulated non-uniform magnetic field, *Langmuir*, 36 (2020) 7724–7740.
[42] M.A. Bijarchi, A. Favakeh, M.B. Shafii, The effect of a non-uniform pulse-width modulated magnetic field with different angles on the swinging ferrofluid droplet formation, *Journal of Industrial and Engineering Chemistry*, 84 (2020) 106-119.
[43] A. Favakeh, M.A. Bijarchi, M.B. Shafii, Ferrofluid droplet formation from a nozzle using alternating magnetic field with different magnetic coil positions, *Journal of Magnetism and Magnetic Materials*, 498 (2020) 166134.
[44] M.A. Bijarchi, A. Favakeh, S. Alborzi, M.B. Shafii, Experimental investigation of on-demand ferrofluid droplet generation in microfluidics using a Pulse-Width Modulation magnetic field with proposed correlation, *Sensors and Actuators B: Chemical*, 329 (2021) 129274.
[45] M.A. Bijarchi, A. Favakeh, E. Sedighi, M.B. Shafii, Ferrofluid droplet manipulation using an adjustable alternating magnetic field, *Sensors and Actuators A: Physical*, 301 (2020) 111753.
[46] C.-Y. Chen, C.-H. Chen, W.-F. Lee, Experiments on breakups of a magnetic fluid drop through a micro-orifice, *Journal of Magnetism and Magnetic Materials*, 321(20) (2009) 3520-3525.
[47] M.L. Steegmans, K.G. Schroën, R.M. Boom, Microfluidic Y-junctions: A robust emulsification system with regard to junction design, *AIChE Journal*, 56(7) (2010) 1946-1949.
[48] C.-W. Chang, Y.-T. Cheng, C.-Y. Tsai, J.-H. Chien, P.-Y. Wang, P.-H. Chen, Periodic flow patterns of the magnetic fluid in microchannel, *Journal of Magnetism and Magnetic Materials*, 310(2) (2007) 2844-2846.
[49] R.E. Rosensweig, *Ferrohydrodynamics*, Courier Corporation, 2013.
[50] Á. Romero-Calvo, G. Cano-Gómez, T.H. Hermans, L.P. Benítez, M.A.H. Gutiérrez, E. Castro-Hernández, Total magnetic force on a ferrofluid droplet in microgravity, *Experimental Thermal and Fluid Science*, 117 (2020) 110124.

ORCID iD

Mohammad Aboutalebi https://orcid.org/0000-0002-4581-1443
Mohammad Behshad Shafii https://orcid.org/0000-0002-6266-8853
Siamak Kazemzadeh Hannani https://orcid.org/0000-0001-6298-0444

How to cite this article: Aboutalebi M., Shafii M.B., Hannani S.K. Numerical Study on the Ferrofluid Droplet Splitting in a T-junction with Branches of Unequal Widths using Asymmetric Magnetic Field, *J. Appl. Comput. Mech.*, 9(2), 2023, 357–370. https://doi.org/10.22055/JACM.2021.36722.2892